TR-82-020

STATISTICAL APPROACH TO THE IDENTIFICATION OF A THREE DIMENSIONAL OBJECT VIEWED FROM RANDOM DIRECTIONS

By

Jun S. Huang and Julius T. Tou
Center for Information Research
University of Florida
July 1982

*This research is supported by the National Science Council of Rep. of China.

** Jun S. Huang is currently at Institute of Information Science, Academia Sinica, Taipei, Taiwan, R.O.C.

ABSTRACT: We consider the situation where a 3-dimensional object is moving in some area and n pictures of this object, $n \geq 2$, are taken in random viewing angles by a camera from an aircraft. Each time when a picture is taken the central position of the object relative to the camera is measured but the orientation of the object can not be determined and is unknown. From these n pictures and the camera's positions we try to identify the object by computer. A parallelepiped is chosen for the identification and a new approach is developed for pattern classifcation based on the distributions of the lengths of edges and the sizes of angles of the parallelepiped. Some distance measures are introduced between the object in pictures and the parallelepiped. These are Kolmogorov-Smirnov statistic, Cramér-von Mises statistic and their generalizations. The probability of misclassification is also discussed. This study has wide applications in military and industry. A brief system architecture for future implementation is discussed here.

Index Terms -- Pattern classification, 3D object, random viewing angles, skeleton, distribution, statistic, parallelepiped.

1. INTRODUCTION

The main problem to be investigated here can be described as follows. A 3-dimensional object, an airplane or a tank or else, is flying in the sky or moving in a field. A camera from an aircraft has taken n pictures of this object, $n \geq 2$. The pictures are taken from random viewing angles and each time when a picture is taken the central position of the object, relative to the camera, is measured but the orientation of the object can not be determined and is unknown. The orientation may change with time. From these n pictures and the information about the camera's positions, can the object be identified? To what extent? What is the probability of misclassification if we already know that the object comes from one of the k, $k \geq 2$, types of objects? Evidently these questions can not be answered easily. But since the computer technology and the theory of statistics advance so fast that the problems related to these questions becomes partly solvable at this time. The main tool to sovle these problems is the modern statistical decision theory. The knowledge-based technique is not considered here. although it provides one way to solve these problems.

The basic idea of solving our problem is to extract some invariant features under the rotation of the given

object. Since the viewing angles are random, we can treat the object as having been subjected to random rotations when the position of the camera is fixed all the time. The invariant features extracted thus are related to geometric probability and integral geometry [1,2,3,4]. In fact what we are interested are the distributions of lengths of edges and sizes of angles of the object when the object is viewed from random angles. From these information we can define some distance measures between the object in pictures and a given object. These distance measures turn out to have very nice properties that they are distribution free and the critical regions for a specified probability of making type one error, in hypothese testing, have been tabulated [5]. Also after some modifications of these distance measures, they can be easily computed.

In many cases, the object considered does not have clear cut of edges and angles. However, for some cases the object can be represented by its skeleton [6, 7] and the skeleton can then be approximated by linear splines with a fixed number of nodes. Thus the object can be characterized by the skeletons of its images. In this case our proposed principle can also be applied. Another way of treating objects without clear cut of edges and angles is by polyhedral approximation. The object's image can be approximated by some polygons and there may be some correspondence between the polygon and the polyhedron. This needs further study.

2. PROCEDURE FOR THE IDENTIFICATION OF A PARALLELEPIPED

To demonstrate our new idea of pattern classification, we begin the study with three tetrahedrons of similar sizes, say a cube, a parallelepiped and a general tetrahedron. A cube can be characterized by the right angles and the equal edge lengths. A parallelepiped can be characterized by the equal sizes of facing angles and the equal lengths of two facing edges. These three objects have similar images frequently, depending on the viewing angles. They are difficult to be distinguished, by just one or very few number of pictures, from each other. Objects that are not tetrahedrons can be distinguished from a tetrahedron easily by just checking their vertex number.

The whole procedure of identifying a parallelepiped with n pictures taken from random viewing angles is sketched in Figure 1, where the procedure contains two subprocesses. One subprocess in right hand side is called the object process which extracts useful information that can be characterized from the parallelepiped. The other in left hand side is called the picture process which extracts information from the pictures. The two processes are merged in the classification procedure.

The object process starts with the given parallelepiped. This parallelepiped is projected onto the picture plane

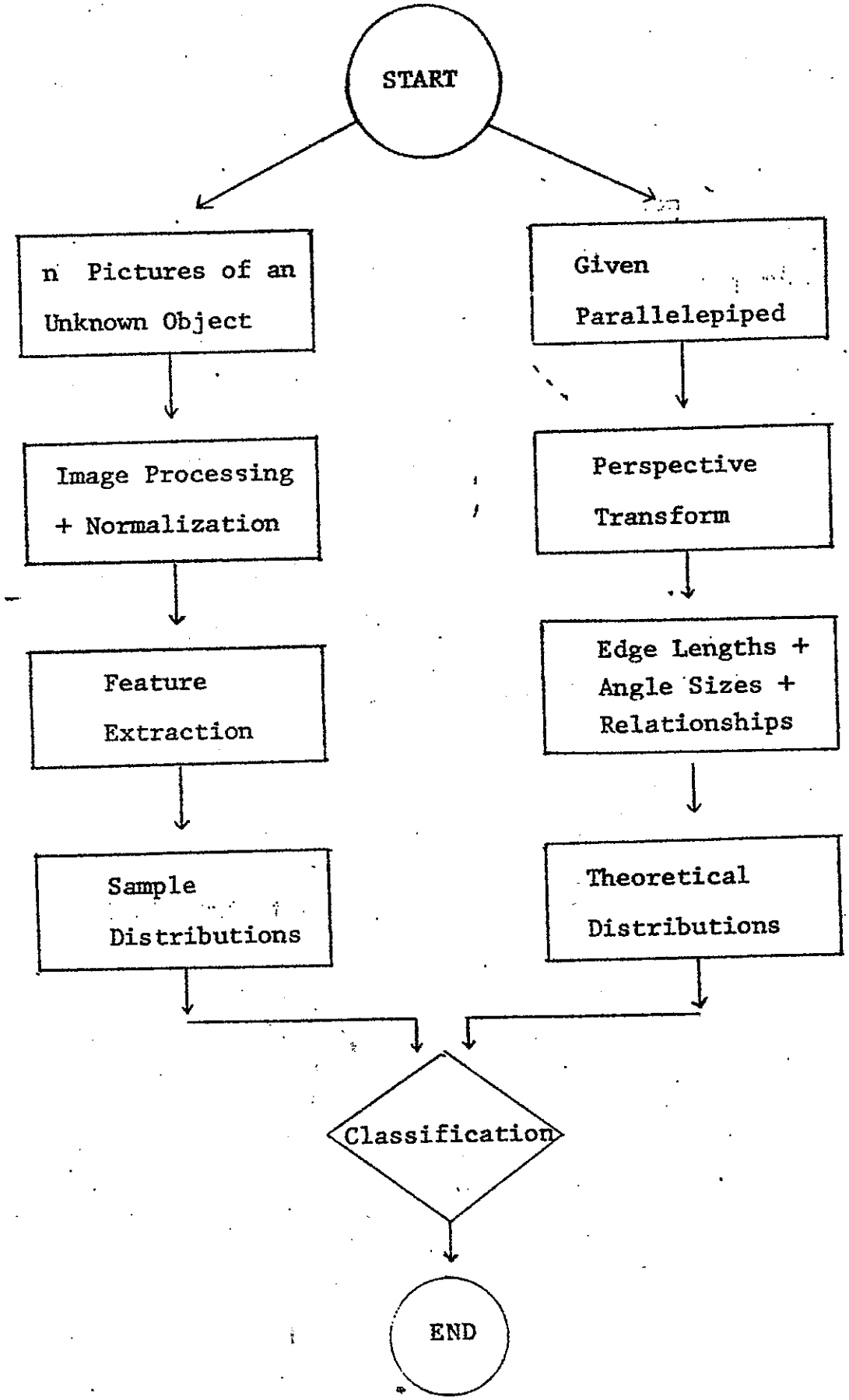

Figure 1. Identification of a Parallelepiped.

through perspective transform that describes the camera's function. The edge lengths and angle sizes of the object's image are evaluated as functions of the viewing angle, and their structural relationship is also kept for later identification. After this step we then treat the viewing angle as a random variable having some specific distribution, say uniform distribution. In this way, the distributions of edge lengths and angle sizes, called theoretical distributions here, can be found and are passed to the classification procedure.

The picture process starts with taking n pictures of the unknown object. The pictures are processed so that the edges and angles in each picture can be detected. The scale and the position of each object's image can be normalized based on the viewing angles and the distances between the camera and the object. Third step is the feature extraction which extracts some useful data from each picture. Generally the extracted data will consist of values of edge lengths and angle sizes in each region of the object's image. Finally we form some sample distributions (or empirical distributions) from all data.

The sample distributions and the theoretical distributions are used to define some distance measures that measure the similarity between the unknown object and the parallelepiped. The classification of the unknown object will be done by the statistical hypothese tests based on these distance measures. Details of the procedure will be discussed in the following sections.

3. THE OBJECT PROCESS

Referring to Figure 2, we consider a camera with focal length f and the gimbal center at the point (x_0, y_0, z_0). The global reference system is denoted by the unprimed (X, Y, Z) coordinates, and is used to locate both the camera and the object point V_p. The camera is moved from the origin, panned through an angle θ horizontally in counter clockwise direction from the Y axis, and tilted through an angle ϕ in an upward direction. The image point V_p' is measured with respect to an image coordinate system (X', Z') of the image plane. Let $V_0 = (x_0, y_0, z_0)$ be the vector from the origin of the global frame to the gimbal center. Let the vector ℓ be constant offset between gimbal center and image plane center, where ℓ is measured in the gimbal coordinate system. Let $\ell = (\ell_1, \ell_2+f, \ell_3)$ so that if the gimbal center were at the lens center, we have

$\ell_1 = \ell_2 = \ell_3 = 0$ and a constant offset of f along the optical axis. Let $V_p = (x, y, z)$ and $V_p' = (x_p', z_p')$. After some computations based upon photogrammetry principles, the relationship between V_p and V_p' is given by the following two equations:

$$x_p' = f \frac{(x-x_0)\cos\theta + (y-y_0)\sin\theta - \ell_1}{-(x-x_0)\cos\phi \sin\theta + (y-y_0)\cos\phi \cos\theta + (z-z_0)\sin\phi - \ell_2}$$

$$z_p' = f \frac{(x-x_0)\sin\phi \sin\theta - (y-y_0)\sin\phi \cos\theta + (z-z_0)\cos\phi - \ell_3}{-(x-x_0)\cos\phi \sin\theta + (y-y_0)\cos\phi \cos\theta + (z-z_0)\sin\phi - \ell_2} \qquad (1)$$

which is called perspective transformation.

In order to solve the problem of identifying an object from pictures taken from random viewing angles, we must normalize the positon of the object, here a parallelepiped, so that equations to be derived later on can be simplified and standardized. Let a parallelepiped be represented by its eight vertices $V_1, V_2, \ldots, V_8$, and let its top surface be formed by V_1, V_2, V_3, V_4 lying on the X - Y plane as shown in Figure 3. Also let the center of the top surface be at the origin. We assume that the camera's gimbal center be at $V_0 = (0, y_0, z_0)$, $y_0 < 0$, $z_0 > 0$, and that the optical axis pass through the origin when the camera aims at the object. The angle between the optical axis and the horizontal line is θ which has negative value here. The angle of

camera's rotation in X - Y plane is θ which has value zero here. Thus Eq.1 becomes

$$x'_p = f \frac{x - \ell_1}{(y-y_0)\cos\phi + (z-z_0)\sin\phi - \ell_2},$$
$$z'_p = f \frac{-(y-y_0)\sin\phi + (z-z_0)\cos\phi - \ell_3}{(y-y_0)\cos\phi + (z-z_0)\sin\phi - \ell_2}. \quad (2)$$

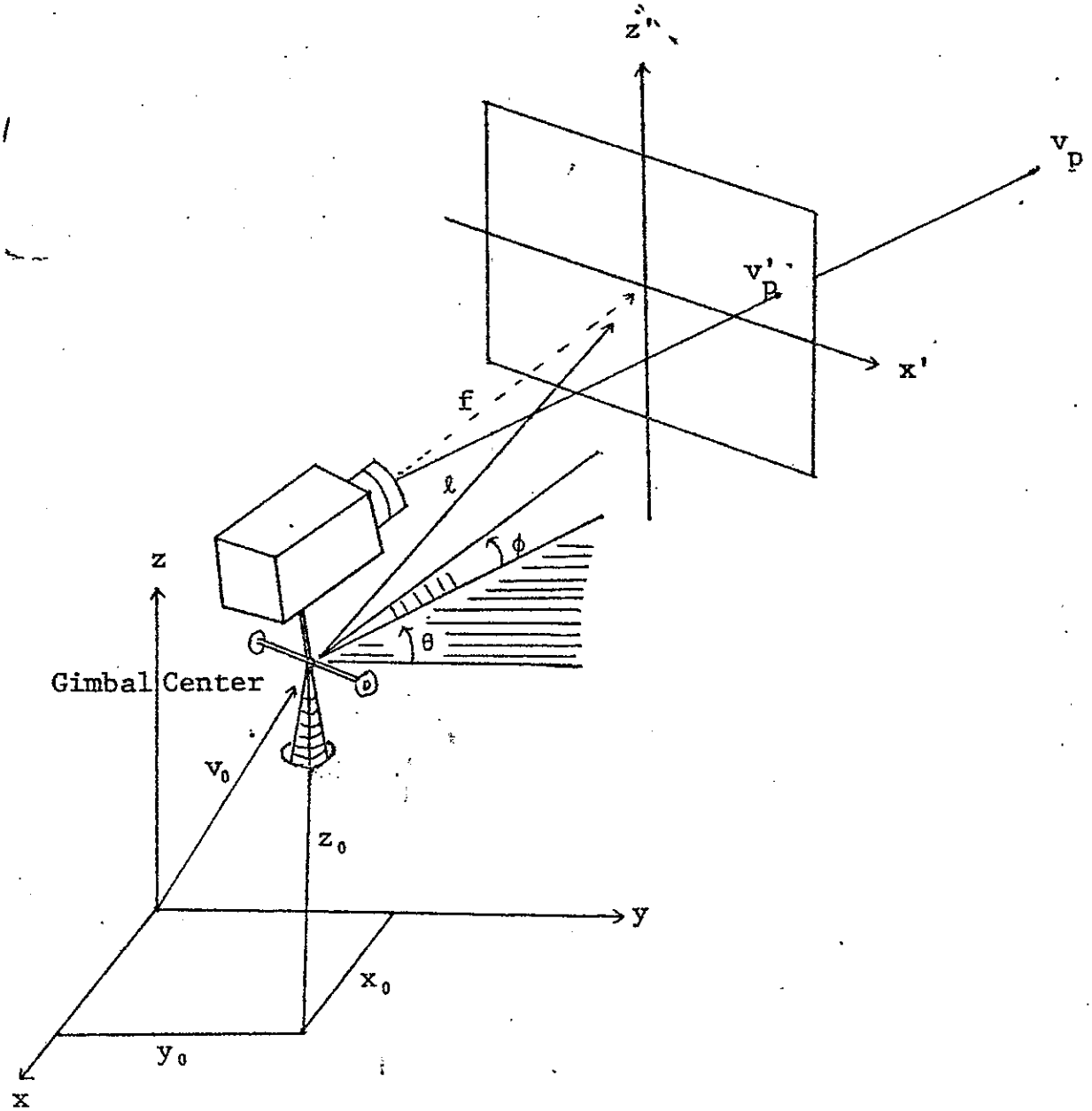

Figure 2. Perspective Transformation With Two Reference Frames.

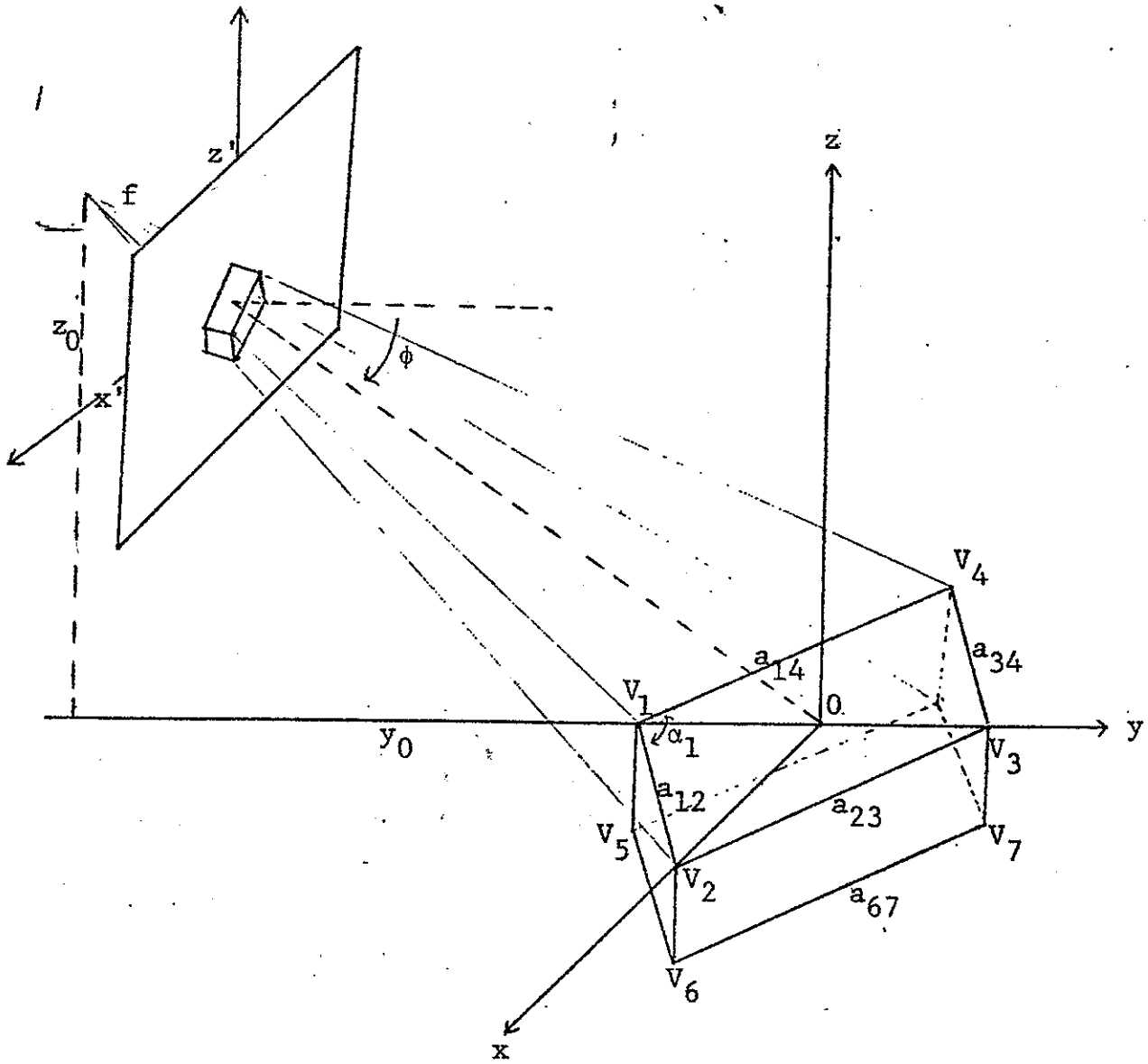

Figure 3. The Picture Frame and the Parallelepiped.

In our consideration ϕ should not be zero since we try to view the object from a spacecraft, and also we try to simplify the problem by first assuming ϕ is fixed all the time and the camera just circles around the object with center on z axis, height of z_0 and a constant distance between the origin and the camera.

Moving the camera to circle around the object and taking pictures at random viewing angles is equivalent to fixing the camera at a specific location and rotating the object with random angles, and then taking pictures. Since we consider ϕ to be fixed, the rotation of the object in this case is a planar rotation on x - y plane. Thus the point (x, y, z) on the object rotates to a point with coordinate (x_1, y_1, z_1) where $z_1 = z$, $x_1 = x\cos\theta + y\sin\theta$ and $y_1 = -x\sin\theta + y\cos\theta$, θ = rotation angle. From this information and Eq.2, we get a relationship between a point on the object after rotation and its projection on the picture plane. The relationship is given by Eq.3:

$$x'_p = f\,\frac{x\cos\theta + y\sin\theta - \ell_1}{(-x\sin\theta + y\cos\theta - y_0)\cos\phi + (z-z_0)\sin\phi - \ell_2}\,,$$

$$z'_p = f\,\frac{(x\sin\theta - y\cos\theta + y_0)\sin\phi + (z-z_0)\cos\phi - \ell_3}{(-x\sin\theta + y\cos\theta - y_0)\cos\phi + (z-z_0)\sin\phi - \ell_2}\,. \qquad (3)$$

From Fig. 3 the edge between V_1 and V_2 is labelled by a_{12} and the edge between V_1 and V_4 by a_{14} and so

on as shown in the figure. After the parallelepiped is projected on the picture plane, the length of each edge and the angle between any pair of adjacent edges will depend on the viewing angle and some will not appear on the picture plane. For example, in Fig.3, the vertice V_1 will give a projection point, say V_1', coming with three edges and three angles. But V_2 will give a point V_2' with only three edges and two angles in the projection. Our further investigation is to find the relationship between the change of θ and the changes of vertices, edges, and the structure of the object.

Let the absolute sign $|\cdot|$ of an edge be its length. The projection of the edge a_{12} is denoted by a_{12}' and it has length $|a_{12}'| = \|V_2' - V_1'\|$. Without loss of generality, let $V_1 = (0, v_1, 0)$ and $V_2 = (v_2, 0, 0)$, $v_1 > 0$, $v_2 > 0$. Then the squared length $|a_{12}'|^2$ of a_{12}' after rotation of an angle θ, is found to be

$$|a_{12}'|^2 = f^2\left\{\left[\frac{v_2\cos\theta - \ell_1}{(-v_2\sin\theta-y_0)\cos\phi-z_0\sin\phi-\ell_2} - \frac{-v_1\sin\theta - \ell_1}{(-v_1\cos\theta-y_0)\cos\phi-z_0\sin\phi-\ell_2}\right]^2\right.$$
$$\left. + \left[\frac{(v_2\sin\theta+y_0)\sin\phi-z_0\cos\phi-\ell_3}{(-v_2\sin\theta-y_0)\cos\phi-z_0\sin\phi-\ell_2} - \frac{(v_1\cos\theta+y_0)\sin\phi-z_0\cos\phi-\ell_3}{(-v_1\cos\theta-y_0)\cos\phi-z_0\sin\phi-\ell_2}\right]^2\right\},$$
$$= f^2\frac{A_1^2 + B_1^2}{[(v_2\sin\theta+y_0)\cos\phi+z_0\sin\phi+\ell_2]^2[(v_1\cos\theta+y_0)\cos\phi+z_0\sin\phi+\ell_2]^2}, \qquad (4)$$

where $A_1 = -v_1v_2\cos\phi + \delta(y_0\cos\phi + z_0\sin\phi + \ell_2)\sin(\theta+\beta) + \delta\ell_1\cos\phi\cos(\theta+\beta)$,

$$B_1 = \delta\cos(\theta+\beta)(z_0 + \ell_2\sin\phi + \ell_3\cos\phi),$$

and $\delta = \sqrt{v_1^2 + v_2^2}$ (i.e. $\delta = |a_{12}|$), $\beta = \tan^{-1}(v_2/v_1)$.

In general we can put $\ell_1 = \ell_2 = \ell_3 = 0$ for simplicity, then

$$|a'_{12}|^2 = f^2 \frac{[\delta z_0\cos(\theta+\beta)]^2 + [v_1v_2\cos\phi+\delta\sin(\theta+\beta)(y_0\cos\phi+z_0\sin\phi)]^2}{[(v_2\sin\theta+y_0)\cos\phi+z_0\sin\phi]^2[(v_1\cos\theta-y_0)\cos\phi-z_0\sin\phi]^2}$$

This formula is very complicated. However we can use the computer to evaluate it and plot a graph when θ changes from 0 to 2π. Two plots are given in Figs.4 and 5 for different values of v_1 and v_2 when $y_0 = -100$, $z_0 = 50$, $\phi = -\pi/6$, $f = 1$ and $\ell_1 = \ell_2 = \ell_3 = 0$.

Similarly we find the image a'_{14} of the edge a_{14} with squared lenght $|a'_{14}|^2$ givne by

$$|a'_{14}|^2 = f^2 \frac{A_2^2 + B_2^2}{[(y_0-v_2\sin\theta)\cos\phi+z_0\sin\phi+\ell_2]^2[(y_0+v_1\cos\theta)\cos\phi+z_0\sin\phi+\ell_2]^2}$$

where $A_2 = v_1v_2\cos\phi-\delta(y_0\cos\phi+z_0\sin\phi+\ell_2)\sin(\theta-\beta)+\delta\ell_1\cos\phi\cos(\theta-\beta)$

and $B_2 = \delta\cos(\theta-\beta)(z_0 + \ell_2\sin\phi+\ell_3\cos\phi)$.

In general $\ell_1 = 0$ then $|a'_{14}|$ evaluated at $-\theta$ is equal to $|a'_{12}|$ evaluated at θ.

Now we can calculate the projection α'_1 of the angle

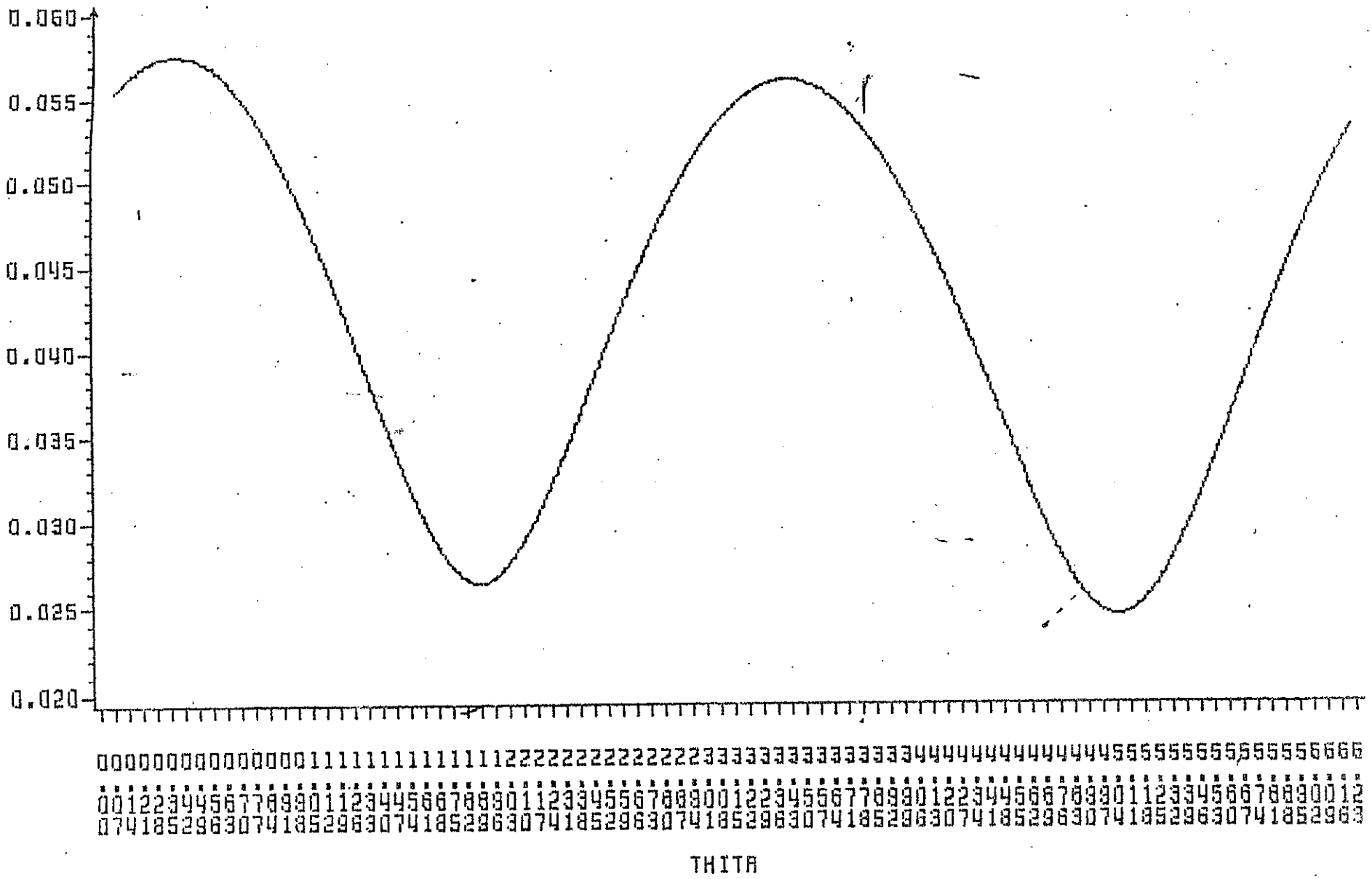

Figure 4. $|a'_{12}|$ vs. θ for $v_1 = 2$, $v_2 = 6$.

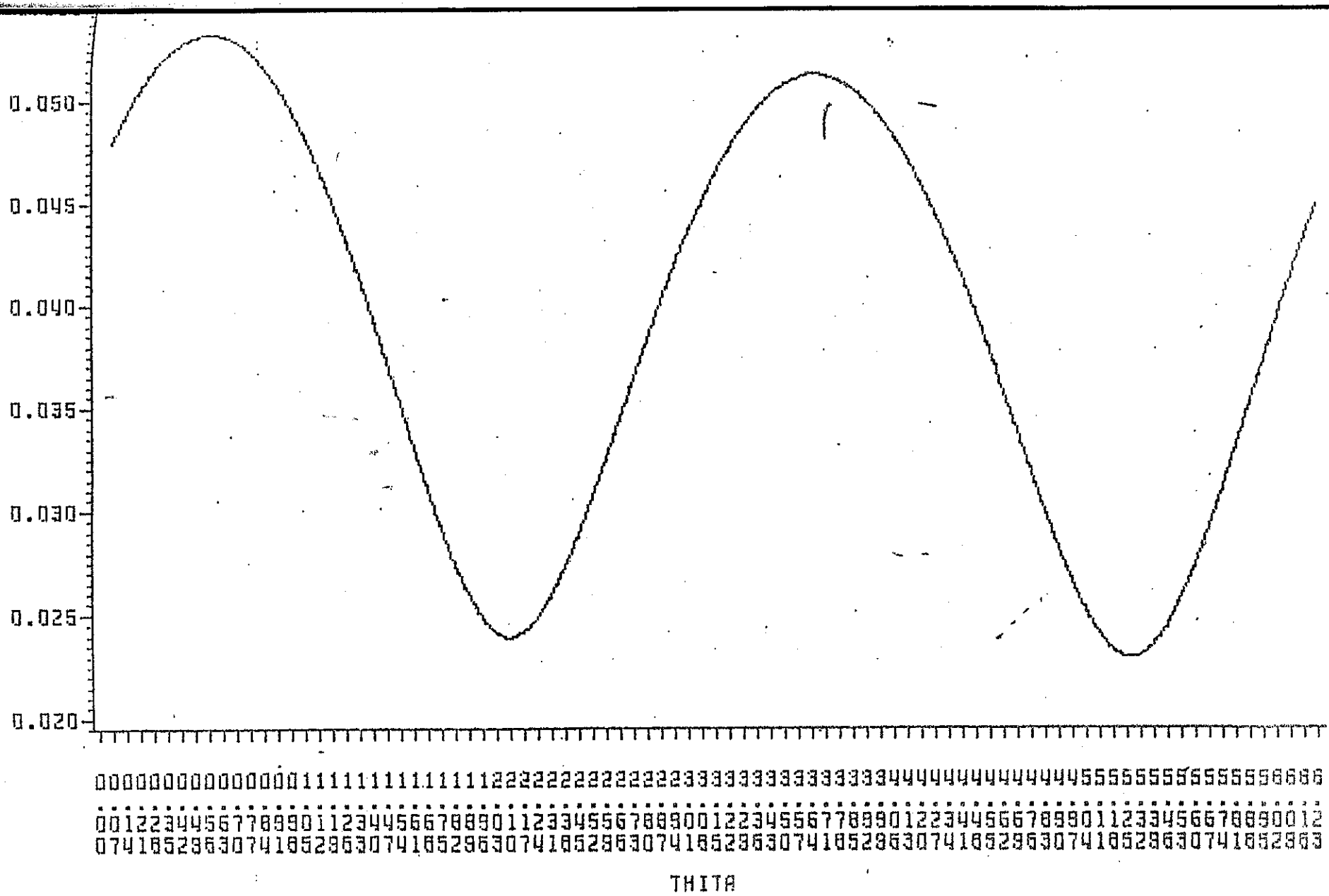

Figure 5. $|a'_{12}|$ vs. θ for $v_1 = 3$, $v_2 = 5$.

α_1 between two edges a_{12} and a_{14}. Since there is one-to-one correspondence between α_1' and $\cos\alpha_1'$ when $0 \le \alpha_1' < \pi$, we shall consider $\cos\alpha_1'$ to be a measure of the angle size, instead of α_1'. The $\cos\alpha_1'$ can be calculated by

$$\cos\alpha_1' = \frac{(V_2'-V_1') \cdot (V_4'-V_1')}{|a_{12}'| \cdot |a_{14}'|} = \frac{A_1A_2 + B_1B_2}{\sqrt{(A_1^2 + B_1^2)(A_2^2 + B_2^2)}} \qquad (5)$$

where $A_i's$ and $B_i's$ are defined as before and the dot sign in the numberator means the inner product of two vectors. Again, we can use computer to evaluate $\cos\alpha_1'$. Three plots have been obtained and are given in Figs.6, 7 and 8, where $f = 1$, $\ell_1 = \ell_2 = \ell_3 = 0$, $y_0 = -100$, $z_0 = 50$, $\phi = -\pi/6$.

In the same way, we can derive all formulas for the rest of image edges and image angles. Most of them are listed below. Formulas for angles are similar to Eq.5

$$|a_{34}'|^2 = |a_{12}'|^2 \quad \text{evaluated at} \quad \theta + \pi$$

$$= f^2 \frac{A_3^2 + B_3^2}{[(-v_2\sin\theta+y_0)\cos\phi+z_0\sin\phi+\ell_2]^2\,[(-v_1\cos\theta-y_0)\cos\phi-z_0\sin\phi+\ell_2]^2}$$

where $A_3 = v_1v_2\cos\phi - \delta(y_0\cos\phi+x_0\sin\phi+\ell_2)\sin(\theta+\beta) + \delta\ell_1\cos\phi\cos(\theta+\beta)$,

and $B_3 = -\delta\cos(\theta+\beta)(z_0+\ell_2\sin\phi+\ell_3\cos\phi)$.

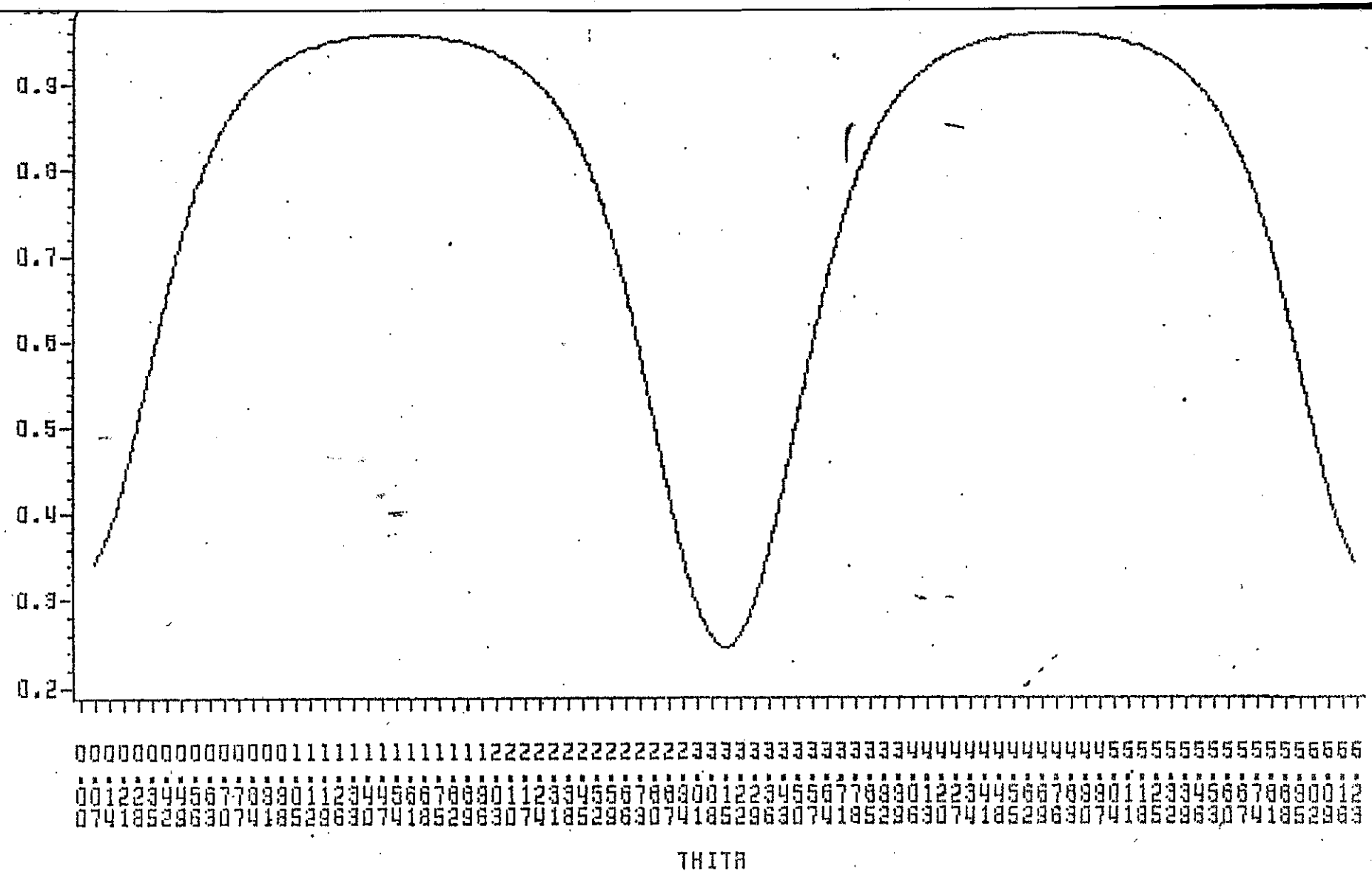

Figure 6. $\cos(\alpha_1')$ vs. θ for $v_1 = 6$, $v_2 = 2$.

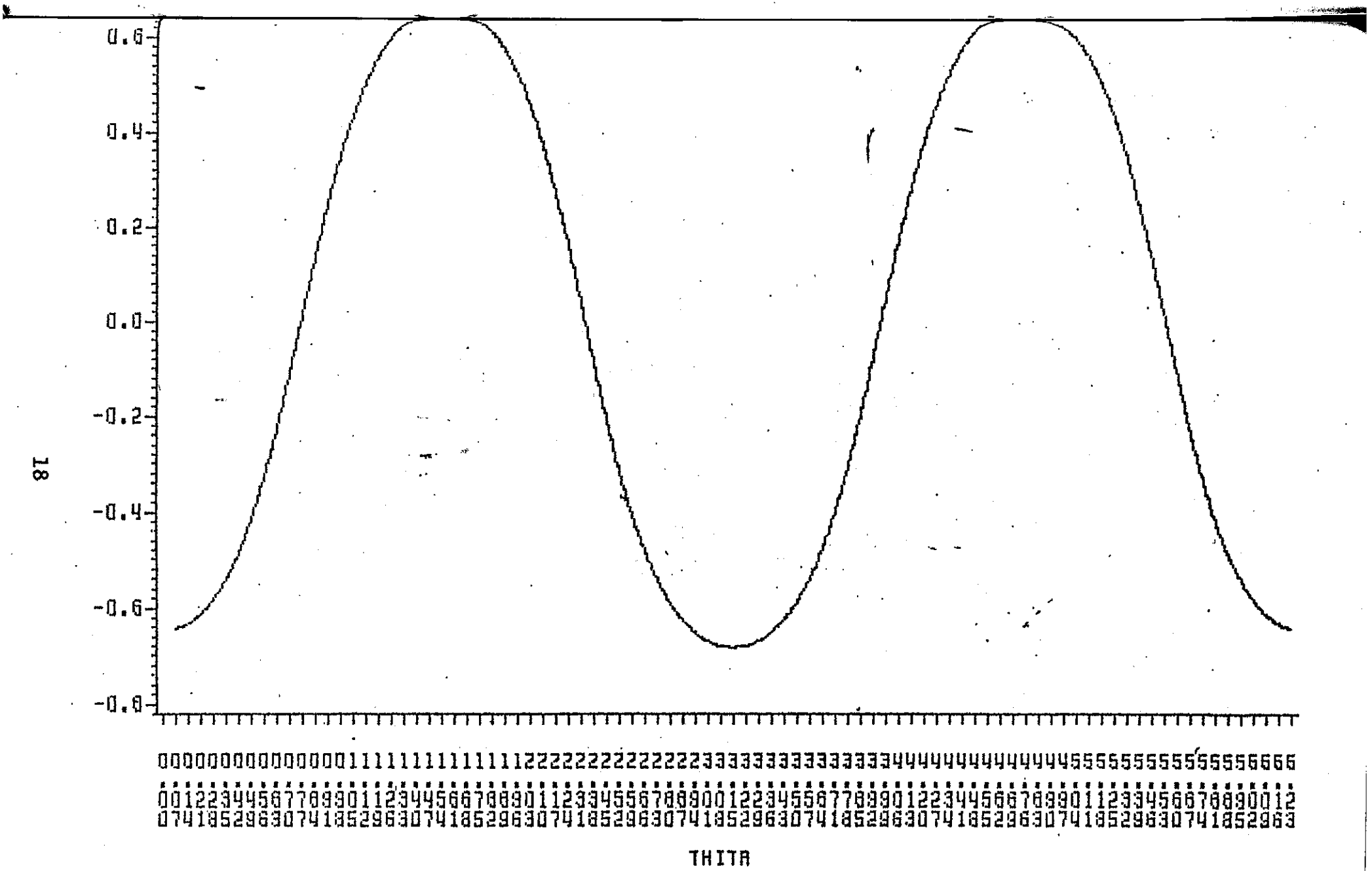

Figure 7. $\cos(\alpha_1')$ vs. θ for $v_1 = 4$, $v_2 = 4$.

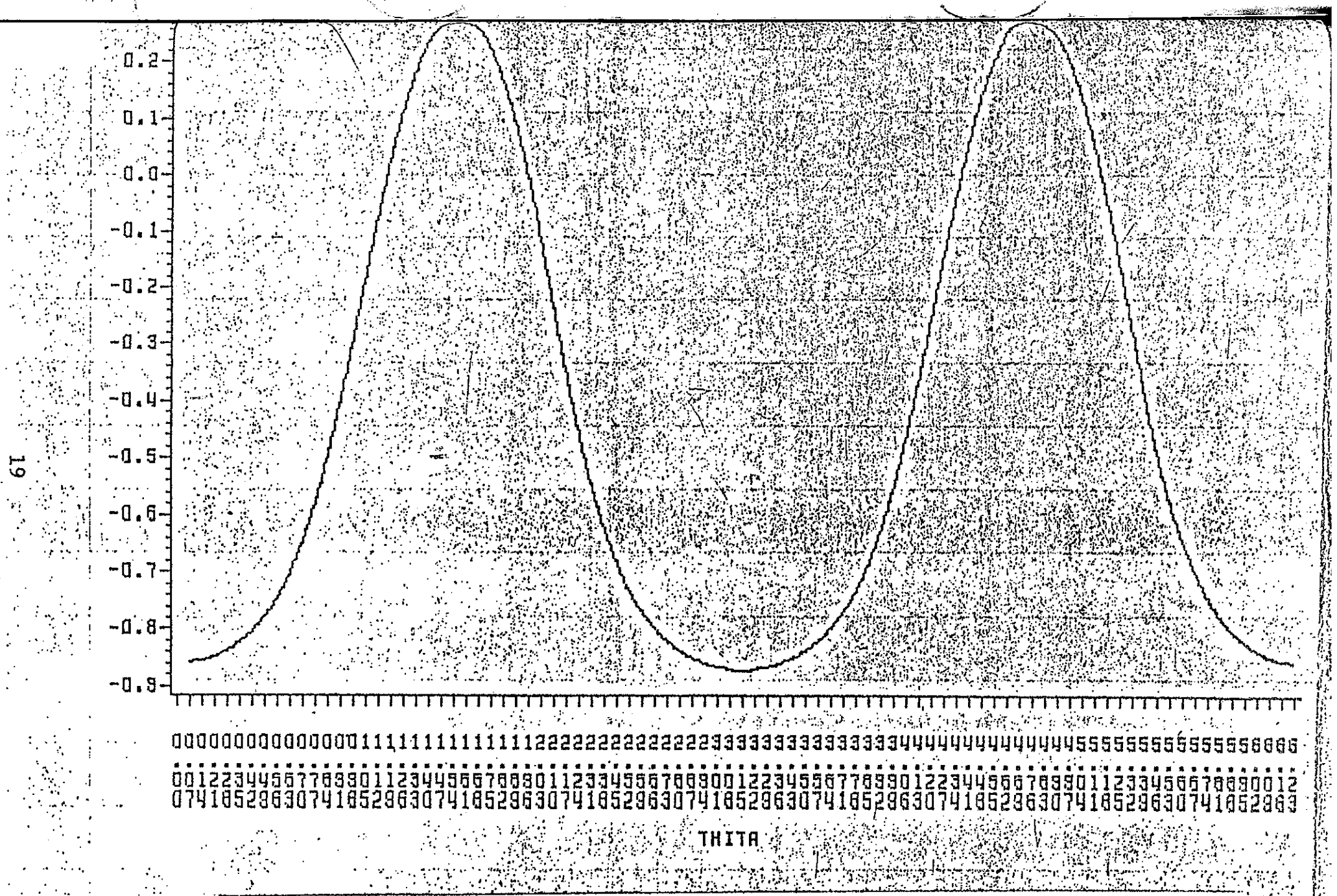

Figure 8. $\cos(\alpha_1')$ vs. θ for $v_1 = 3$, $v_2 = 5$.

$|a'_{23}|^2 = |a'_{14}|^2$ evaluated at $\theta + \pi$

$$= f^2(A_4^2 + B_4^2)/[[(y_0+v_2\sin\theta)\cos\phi+z_0\sin\phi+\ell_2]^2[(y_0-v_1\cos\theta)\cos\phi + z_0\sin\phi+\ell_2]^2,$$

where $A_4 = v_1v_2\cos\phi + \delta(y_0\cos\phi+z_0\sin\phi+\ell_2)\sin(\theta-\beta) - \delta\ell_1\cos\phi\cos(\theta-\beta)$,

and $B_4 = -\delta\cos(\theta-\beta)(z_0+\ell_2\sin\phi+\ell_3\cos\phi)$.

The angle α'_2 has value given by

$$\cos\alpha'_2 = (A_3A_4 + B_3B_4)/\sqrt{(A_3^2 + B_3^2)(A_4^2 + B_4^2)}\ .$$

Let $V_5 = (u, -v_1, -v_3)$, $v_3 > 0$. Then the edge a_{15} between two vertices V_1 and V_5 has an image edge a'_{15} with length a'_{15}, and

$$|a'_{15}|^2 = f^2\left\{\frac{A_5^2 + B_5^2}{[(-v_1\cos\theta-y_0)\cos\phi-z_0\sin\phi-\ell_2]^2[(-u\sin\theta-v_1\cos\theta-y_0)\cos\phi-(v_3+z_0)\sin\phi-\ell_2]^2}\right\}$$

where $A_5 = uv_1\cos\phi + v_1v_3\sin\theta\sin\phi+u\cos\theta(\ell_2+y_0\cos\phi+z_0\sin\phi) + \ell_1(u\sin\theta\cos\phi+v_3\sin\phi)$,

and $B_5 = u\sin\theta(z_0+\ell_2\sin\phi+\ell_3\cos\phi) - v_1v_3\cos\theta$

$$- v_3(y_0-\ell_2\cos\phi-\ell_3\sin\phi).$$

Let $V_6 = (u+v_2,\ 0,\ -v_3)$. Then the edge a_{26} between V_2 and V_6 has an image edge a'_{26} with length $|a'_{26}|$ and

$$|a'_{26}|^2 = f^2\left\{\frac{A_6^2 + B_6^2}{[-(v_2\sin\theta+y_0)\cos\phi-z_0\sin\phi-\ell_2]^2[[-(u+v_2)\sin\theta-y_0]\cos\phi-(v_3+z_0)\sin\phi-\ell_2]^2}\right\}$$

where $A_6 = -v_2v_3\cos\theta\sin\phi + u\cos\theta(\ell_2+y_0\cos\phi+z_0\sin\phi)$

$$+ \ell_1(u\sin\theta\cos\phi+v_3\sin\phi),$$

and $B_6 = u\sin\theta(z_0+\ell_2\sin\phi+\ell_3\cos\phi) - v_2v_3\sin\theta$

$$- v_3(y_0-\ell_2\cos\phi-\ell_3\sin\phi).$$

The edge a_{56} between V_5 and V_6 has an image a'_{56} with length $|a'_{56}|$, and

$$|a'_{56}|^2 = f^2\left\{\frac{A_7^2 + B_7^2}{[(u\sin\theta+v_1\cos\theta+y_0)\cos\phi+(v_3+z_0)\sin\phi+\ell_2]^2[[(u+v_2)\sin\theta+y_0]\cos\phi+(v_3+z_0)\sin\phi+\ell_2]^2}\right\}$$

where $A_7 = v_1(u+v_2)\cos\phi + (v_2v_3\cos\theta+v_1v_3\sin\theta)\sin\phi +$

$$(v_2\cos\theta+v_1\sin\theta)(\ell_2+y_0\cos\phi+z_0\sin\phi) +$$

$$\ell_1(v_2\sin\theta\cos\phi - v_1\cos\theta\cos\phi),$$

$$B_7 = (v_2\sin\theta - v_1\cos\theta)(z_0 + \ell_2\sin\phi + \ell_3\cos\phi) + v_2v_3\sin\theta - v_1v_3\cos\theta .$$

The edge a_{58} between V_5 and V_8 has an image a'_{58} with length $|a'_{58}|$, and

$$|a'_{58}|^2 = f^2\left\{\frac{A_8^2 + B_8^2}{[(u\sin\theta + v_1\cos\theta + y_0)\cos\phi + (v_3+z_0)\sin\phi + \ell_2]^2\{[(u-v_2)\sin\theta + y_0]\cos\phi + (v_3+z_0)\sin\phi + \ell_2\}^2}\right\}$$

where $A_8 = -v_1(u-v_2)\cos\phi + [v_2v_3\cos\theta - v_1v_3\sin\theta]\sin\phi + [v_2\cos\theta - v_1\sin\theta][\ell_2 + y_0\cos\phi + z_0\sin\phi] + \ell_1[v_2\sin\theta\cos\phi + v_1\cos\theta\cos\phi]$,

and $B_8 = (v_2\sin\theta + v_1\cos\theta)(z_0 + \ell_2\sin\phi + \ell_3\cos\phi) + v_2v_3\sin\theta + v_1v_3\cos\theta$.

Please note that for some values of θ we can not see a'_{56}, a'_{58}, a'_{15}, a'_{26} and a'_{48} in the picture. Thus these image edges are defined only on some subrange, say $[-\psi, \psi)$, of θ where ψ can be found geometrically from Fig. 3 and is the solution of the equation $(y_0\cos\psi - v_1)^2 = \cos^2\beta(y_0^2 + v_1^2 - 2y_0v_1\cos\psi)$.

After having found the edge lengths and angle sizes as functions of θ, we then assume θ has a specified distribution, say uniform $[-\pi, \pi)$, and find the distributions of

edge lengths and angle sizes. This can be done only by the computer since the formulas we derived above are all nonlinear functions of θ. In fact, let Y_i be the random variable of the i^{th} edge length or i^{th} angle size where i is an index of a specified ordering. Let y_i be the value of Y_i and $y_i = g_i(\theta)$, where g_i is one of the formulas given above. Then the distribution of Y_i is given by

$$G_i(t) = P(Y_i \leq t) = P(\theta : g_i(\theta) \leq t). \qquad (6)$$

The right hand side is evaluated usually by the lengths of two or three subintervals of $[0, 2\pi)$ or $[-\psi, \psi)$ as shown in Figs. 4,5,6,7, and 8. These distributions $G_i(t)$, $i = 1, 2, \ldots,$ are called theoretical distributions of edges and angles of the given parallelepiped. These distributions characterise the structure of the parallelepiped. An example is given when $v_1 = 6$, $v_2 = 2$. Plot of g_1 is given in Fig. 9 and the corresponding distribution G_1 is given in Fig.10. All computing programs are listed in Appendices A and B.

4. THE PICTURE PROCESS

The picture process starts with n pictures of an unknown object. Each picture is then preprocessed to find

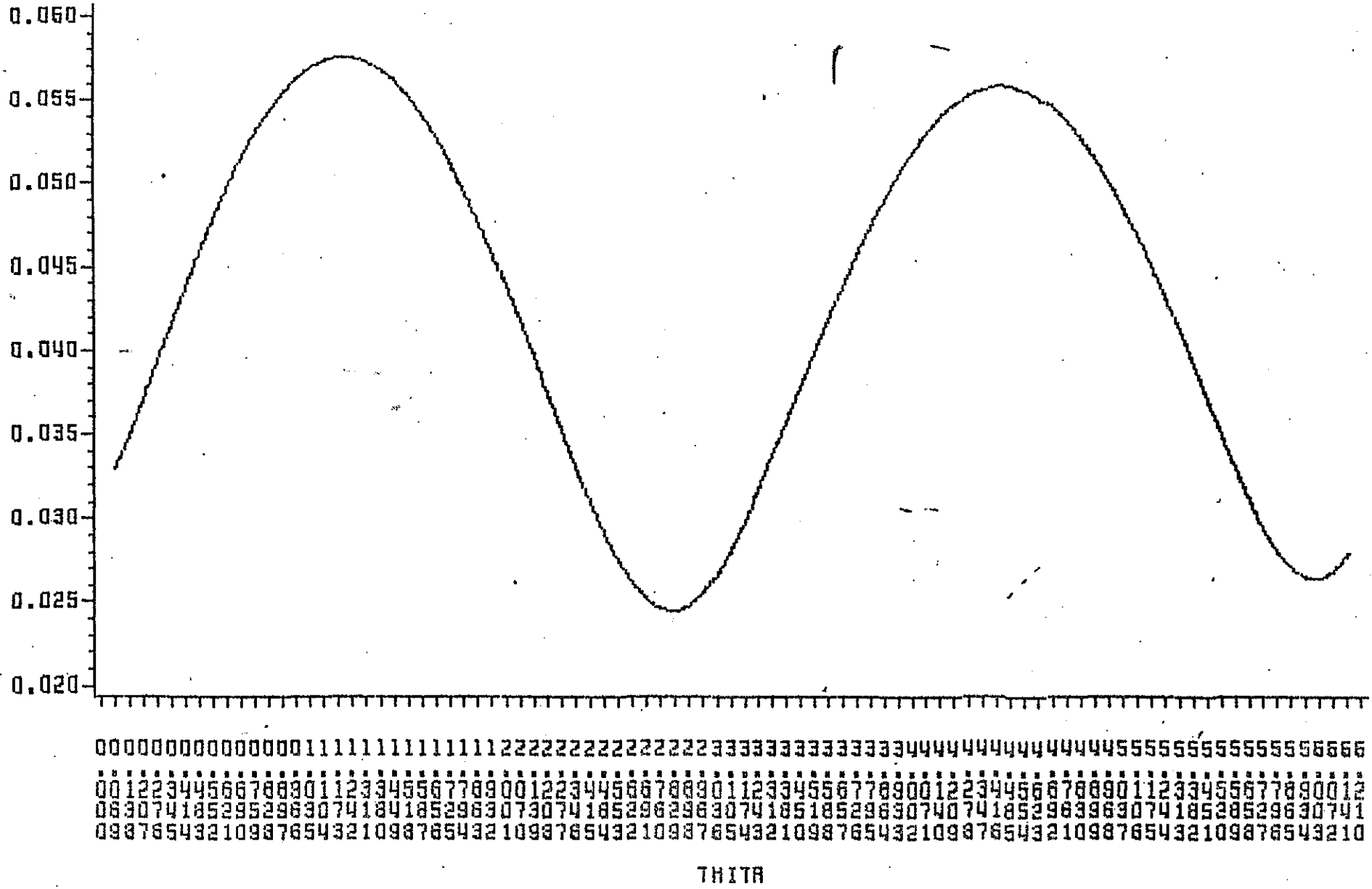

Figure 9. $|a'_{12}|$ vs. θ for $v_1 = 6$, $v_2 = 2$.

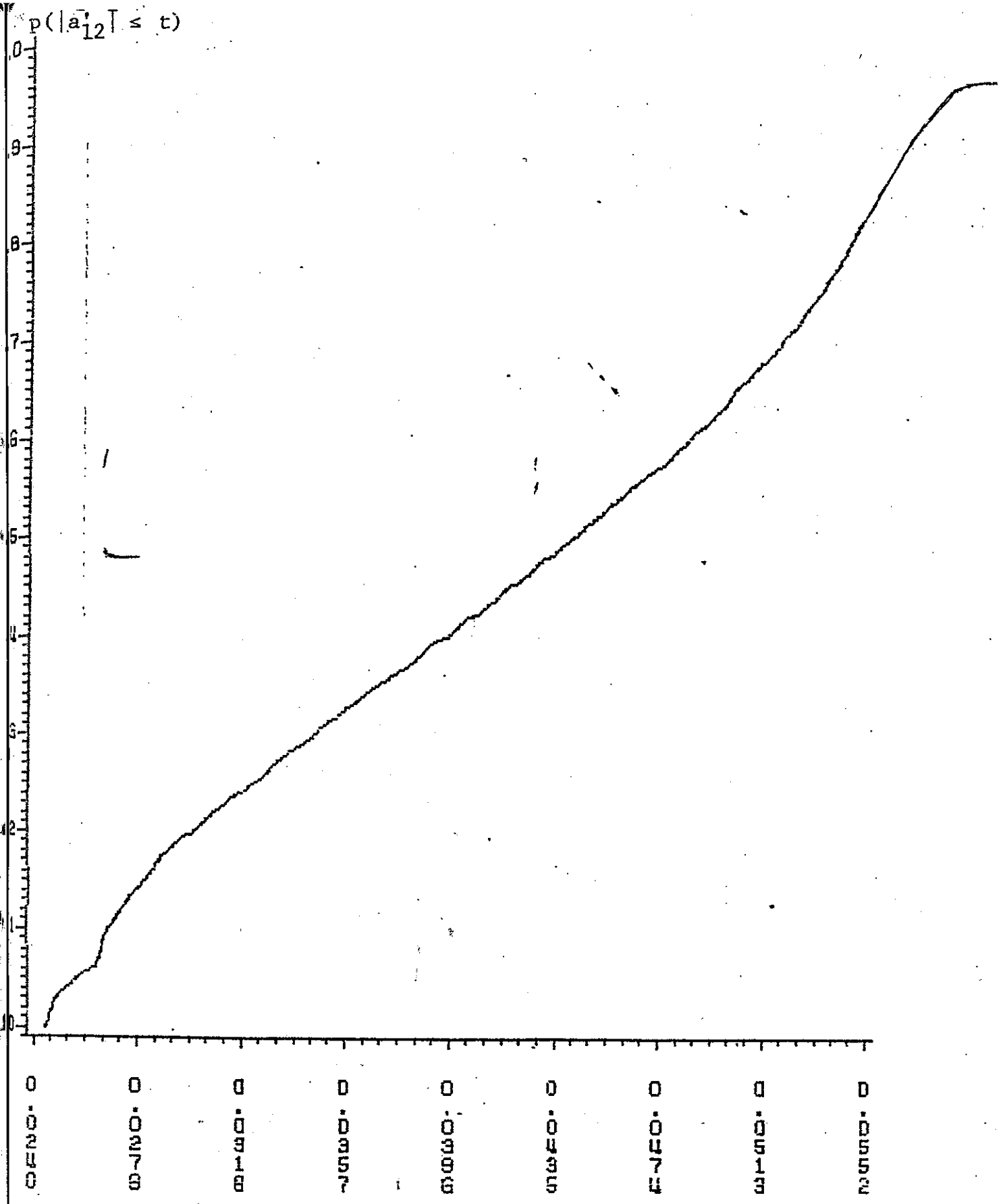

Figure 10. Distribution of $|a'_{12}|$, i.e. G_1 .

the vertices and edges of the object's image. The scale of each object's image will be normalized based on the distance between the camera and the unknown object. The position of the object's image will be shifted so that the image is compatible with Fig. 3. That is, the center of the top region of the object's image is shifted to the origin of the picture coordinate system. The normalization and image processing certainly take some computing time.

Feature extraction from pictures plays the critical role in pattern recognition. After having found the edges, vertices and angles of the object's image, it is not hard to locate the three (or two, in case of noise corruption) regions of the object's image. We call these three regions top region, side region and faced region. The 14 features to be extracted from each picture are defined as follows:

1. Sum of all edge lengths in top region.
2. Sum of all pairwise differences of adjacent edge lengths in top region.
3. Sum of all angle sizes (in cosine values) in top region.
4. Sum of all pairwise differences of adjacent angle sizes in top region.
5. Sum of all vertical edge lengths.
6. Sum of all edge lengths at the bottom.
7. Sum of all edge lengths in the faced region.
8. Sum of all angle sizes (in cosine) in the faced region.

9. Sum of all pairwise differences of adjacent angle sizes in the faced region.

10. Sum of all edge lengths in the side region.

11. Sum of all angle sizes (in cosine) in the side region.

12. Sum of all pairwise differences of adjacent angle sizes in the side region.

13. $\sum_{i=1}^{P} |\Delta x_i|/P$, where $|\Delta x_i|$ is the absolute value of the difference between any two facing edges in each region and p is the number of $|\Delta x_i|$'s; $p = 6$ in most cases and $p = 4$ if the side region can not be detected

14. $\sum_{i=1}^{P} |\Delta \alpha_i|/P$, where $|\Delta \alpha_i|$ is the absolute value of the difference between any two facing angles in each region; p is defined as before.

If the unknown object is still a parallelepiped but with different angle sizes, then features 3,4,5,6,11,12 will give the information of the difference. If the deformed (unknown) object is not a parallelepiped, then features 13 and 14 will give most of the information of the difference. The other features will still contribute some information on the difference. If the object is deformed to such a degree that in the picture we can not

detect one of the 4 vertices, say in the top region, then we do not need these 14 features to make classification. We simply just say that the number of vertices is different from that of a parallelepiped so this object to be classified is surely not a parallelepiped.

After having extracted useful feature data from n pictures, we then form the sample distribution (or empirical distribution) of each feature. Let $X_{i1}, X_{i2}, \ldots, X_{in}$ be the sample data from the i^{th} feature, $i = 1, 2, \ldots, 14$. Then the sample distribution for feature i is defined as

$$F_i(t) = \frac{1}{n} \sum_{j=1}^{n} 1_{(-\infty, t]}(X_{ij}) , \qquad (7)$$

where $1_{(-\infty, t]}$ is an indicator function of the interval $(-\infty, t]$. These sample distributions F_i, $i = 1, 2, \ldots, 14$ will be used to compare the corresponding theoretical distributions discussed in section 3 for the classification.

5. PATTERN CLASSIFICATION

Since given a picture we can not identify which edge comes from a particular edge of the object, any value (observation) from feature 1 has a distribution depends on $G_1(t)$, $G_2(t)$, $G_3(t)$, and $G_4(t)$ where G_1, G_2, G_3 and G_4 are from Eq.6 and are distributions of $|a'_{12}|$, $|a'_{14}|$,

$|a'_{23}|$, $|a'_{34}|$, respectively. Here $G_1 = G_4$ and $G_2 = G_3$ by symmetry. Similarly we can get the distributions of other features. These distributions take much time to evaluate and should be done by the help of computer.

The classification will be based on the distance measures, to be defined in the following, between the unknown object and the given parallelepiped. The distance measures come from the comparisons of the sample distribution (Eq.7) and the mixture distributions of all features. Fortunately, these distance measures are distribution free and their critical values are well tabulated by statisticians. Some further simplifications of these measures have been developed in recent years by Stephens [8].

For feature i, $F_i(t)$ is its sample distribution, and here we denote $H_i(t)$ to be its theoretical distribution that can be obtained from the feature definition and similar methods in computing Eq. (6). Two distance measures are described as follows.

1. $d_i^{(1)} = \sup_{-\infty<t<\infty} |F_i(t) - H_i(t)|$, the Kolmogorov's statistic.

2. $d_i^{(2)} = n \int_{-\infty}^{\infty} (F_i(t) - H_i(t))^2 w(H_i(t)) dH_i(t)$, where w is a proper weighting function. If $w(\cdot) \equiv 1$, then $d_i^{(2)}$ is called Cramér-von Mises statistic. If $w(u) = 1/[u(1-u)]$, $0 < u < 1$, then $d_i^{(2)}$ is called Anderson-Darling statistic.

Since the computations of $d_i^{(1)}$ and $d_i^{(2)}$ involue large number of operations when the sample size is large, and since in general applications large sample size is too expensive for processing, the distance measures $d_i^{(1)}$ and $d_i^{(2)}$ should be modified to be more reliable when the sample size is small. Stephens has modified $d_i^{(1)}$ and $d_i^{(2)}$ and has tabulated the critical values of them in [5].

From Eq.7, let $x_{(i1)} \leq x_{(i2)} \leq \ldots \leq x_{(in)}$ be the order statistic of $X_{i1}, X_{i2}, \ldots, X_{in}$. Let $Z_{(j)} = H_i(x_{(ij)})$, $j = 1, 2, \ldots, n$. Five modified statistics from $d_i^{(1)}$ and $d_i^{(2)}$ are used in practices and are listed below.

(a) The Kolmogorov-Smirnov statistics D^+, D^- and D, where

$$D^+ = \max_{1 \leq i \leq n} [i/n - Z_{(i)}], \quad D^- = \max_{1 \leq i \leq n} [Z_{(i)} - (i-1)/n],$$

$$D = \max [D^+, D^-].$$

(b) The Cramér-von Mises statistic, W^2, where

$$W^2 = \sum_{i=1}^{n} \{Z_{(i)} - (2i - 1)/(2n)\}^2 + \frac{1}{12n} .$$

(c) The Kuiper statistic, V, where

$$V = D^+ + D^- .$$

(d) The Watson statistic, U^2, where

$$U^2 = W^2 - n(\bar{z} - 0.5)^2 \ ;$$

$\bar{z}$ is the sample mean of the $z_{(i)}$, $i = 1,2, \ldots n$.

(e) The Anderson-Darling statistic, A, where

$$A = (-[\sum_{i=1}^{n} (2i-1)\{\log Z_{(i)} + \log(1-Z_{(n+1-i)})\}]/n) - n.$$

Each of these five statistics is then modified, for finite sample size correction, as shown in column 2 of Table 1 (reproduced from [5]), where it contains the approximate critical values of five statistics for certain values of α, probability of type 1 error.

Table 1 Modifications yielding approximate percentage points for the statistics D, V, W^2, U^2 and A in finite samples of n observations

Statistic	Modified forms $T(D^+), T(D), T(V)$, etc.	Upper percentage points for modified T				
		15.0	10.0	5.0	2.5	1.0
$D^+(D^-)$	$D^+(\sqrt{n}+0.12+0.11/\sqrt{n})$	0.973	1.073	1.224	1.358	1.518
D	$D(\sqrt{n}+0.12+0.11/\sqrt{n})$	1.138	1.224	1.358	1.480	1.628
V	$V(\sqrt{n}+0.155+0.24/\sqrt{n})$	1.537	1.620	1.747	1.862	2.001
W^2	$(W^2-0.4/n+0.6/n^2)(1.0+1.0/n)$	0.284	0.347	0.461	0.581	0.743
U^2	$(U^2-0.1/n+0.1/n^2)(1.0+0.8/n)$	0.131	0.152	0.187	0.221	0.267
A	For all $n \geq 5$:*	1.61	1.933	2.492	3.020	3.857

* Marshall (1958) showed that the distribution of A for n = 1 gives results remarkably close to the asymptotic ones, at least in the upper tail. To fill the gap Stephens

carried out a Monte Carlo study for $n = 5$ and found the upper tail asymptotic points to be very close to the corresponding Monte Carlo points.

To make classification, we formulate two hypotheses:

(1). the null hypothese, H_0: the unknown object is the given parallelepiped;

(2) the alternative hypothese, H_a: the unknown object is not the given parallelepiped.

We specify α, the probability of type 1 error, say $\alpha = .01$ or $.05$. Pick up percentage points from Table 1, say Z_α. Then we reject H_0 if the calculated statistic, say $D(\sqrt{n} + 0.12 + 0.11/\sqrt{n})$ is greater than Z_α for some feature i, $1 \le i \le 14$. Note: if we choose D as the classification statistic, then all features should use D. Here we do not use multiple comparsion procedures or analysis of variance since the observations are not all independent for all features.

If we already know that the unknown object comes from one of k types of objects, $k \ge 2$, then we can classify the unknown object into the j^{th} type if the weighted sum of all feature distances (statistics), from the sample data to the j^{th} type of objects, is mininum among all k weighted sums.

6. DISCUSSIONS

We have shown a new classification technique by fitting sample feature distributions with the theoretical distributions of a parallelepiped's edge lengths and angle sizes.

The generalization of our proposed principle to the more general objects is not trivial. For some classes of objects with clear cuts of edges and angles say polyhedrons, our principle can be easily applied. But most 3D objects do not have clear cut of edges and angles. However in many cases we can use polyhedral approximation to the object of interest. Also in some cases we can use skeleton to represent the topological property of the object and the skeleton can be approximated by linear spline of fixed number of nodes (see [6], [7]). These approximations need more study.

An obvious application is in industrial automatic inspection and part selection, where streams of products are coming out with random orientations. The deformed products are classified into defectives. We can fix the camera at a specified location and take pictures of a particular product (the camera should keep tracking of the product). Then we can use the procedure discussed above to make classification.

The computation in the picture process is time critical as oppose to that of the object process which does not require

real time calculations. Given n pictures in the picture process, the image processing, feature extraction, and normal normalization are complex operations. These operations can be processed in parallel by using conventional single instruction multiple data (SIMD) architectures (see [9]). Th modularity exists in the architecture will allow an increasin large number of n if desired.

Aknowledgement. We appreciate Professor Mark Yang of the Departmetn of Statistics, University of Florida, to point out this problem to us. We also thank Professor Y. C. Chow of the Department of Computer and Information Science to give us some valuable comments.

REFERENCES

[1] A. B. J. Novikoff, "Integral geometry as a tool in pattern perception", in Principles of Self-Organization (H. von Foerster and G. W. Zopf, eds.). pp.347-368, Pergamon, N. Y. 1962.

[2] G. H. Ball, "An invariant input for a pattern recognition machine". Ph.D. Thesis. Dept. of Electrical Engineering, Stanford. Univ., 1962.

[3] E. Wong and J. A. Steppe, "Invariant recegnition of geometric shapes", in Methodologies of Pattern Recognition. Watanabe, ed., Academic Press, N.Y., 1969.

[4] H, Solomon, Geometric Probability, SIAM series in Appl. Math., 1978.

[5] E. Pearson and H. Hartley, Biometrika Tables for Statisticians, Vol. II, Cambrige University Press, London, 19.

[6] S. Srihari, "Representation of three dimensional digital images", ACM computing Survey, Vol.13, No.4, pp.399-429 1981.

[7] Y. Tsao and K. S. Fu, "A parallel thinning algorithm for 3-D pictures", Comput. Graph. Image Processing, 1981.

[8] M. A. Stephens, "Use of the Kolmogorov-Smirnov, Cramér-von Mises and related statistics without extensive tables, J. R. Statist. Soc. B 32, 115-22, 1970.

[9] L. J. Siegel, H. J. Siegel and A. E. Feather, "Parallel processing approaches to image correlation", IEEE Transactions on Computers, Vol. C-31, No.3, 1982.

Appendix A. SAS plot of $|a'_{12}|$ and $\cos\alpha'_1$

```
                                                    S T A T I S T I C A L   A N A L Y S

OTE: THE JOB TEST HAS BEEN RUN UNDER RELEASE 79.6 OF SAS AT NORTHEAST REGION

*************************************************************
  YOU ARE RUNNING SAS 79.6 WHICH BECAME THE                  *
  DEFAULT VERSION ON JUNE 21, 1982.                          *
                                                             *
  THE GOULD DEVICE DRIVER (DEVICE=GOULD) IS NOW              *
  WORKING.                                                   *
                                                             *
  THE SASDOC HANDOUT LISTS CURRENT DOCUMENTATION             *
  FOR SAS 79.6.  THERE IS A LIST OF PROBLEMS THAT            *
  HAVE BEEN FIXED AND NEW FEATURES THAT ARE AVAIL-           *
  ABLE.  THESE CAN BE OBTAINED FROM THE CIRCA                *
  CONSULTANT IN 411 WEIL HALL.                               *
                                                  SEB  6/28/82  *
*************************************************************


1          DATA ONE ;
2          V1=6; V2=2;
3          DEL=SQRT(V1**2+V2**2);
4          BETA=ATAN(V2/V1);
5          YO=-100.; ZO=50; FI=-3.14159/6;
6          HSU=YO*COS(FI) + ZO*SIN(FI);
7          DO I=1 TO 90;
8          THITA=2*3.14159*I/90.;
9          A1=-V1*V2*COS(FI)-DEL*HSU*SIN(THITA+BETA);
10         B1=DEL*COS(THITA+BETA)*ZO;
11         A2=V1*V2*COS(FI)-DEL*HSU*SIN(THITA-BETA);
12         B2=DEL*COS(THITA-BETA)*ZO;
13         Y=(A1*A2+B1*B2)/SQRT((A1*A1+B1*B1)*(A2*A2+B2*B2));
14         OUTPUT; END;
15         GOPTIONS DEVICE=GRX ROTATE ;

NOTE: DATA SET WORK.ONE HAS 90 OBSERVATIONS AND 15 VARIABLES.  153 OBS/TRK.
NOTE: THE DATA STATEMENT USED 0.12 SECONDS AND 192K.

16         PROC GPLOT ;
17          PLOT Y*THITA/HAXIS = 0 TO 6.28318 BY .07 CAXIS=BLACK;
18         SYMBOL1 I=SPLINE ;

NOTE: WARNING! DEVICE DRIVER AND PROCEDURE ARE NOT
      AT THE SAME LEVEL.  ERRORS MAY OCCUR.  BEWARE.
      DRIVER=02/27/81  PROC=03/26/82
NOTE: THE PROCEDURE GPLOT USED 0.37 SECONDS AND 300K.


NOTE: SAS INSTITUTE INC.
      SAS CIRCLE
      BOX 8000
      CARY, N.C.  27511-8000
```

Appendix B. Program for converting $|a'_{12}|$ into distribution function.

```
V G LEVEL  21                    MAIN                    DATE = 82217          12/02/26

      DIMENSION THI(400),Y(400),A(91),D(91),E(91),F(91),G(91)
      READ(2,1)(THI(I),Y(I),I=1,400)
1     FORMAT(2F12.9)
      CALL MAX(Y,A1,A2)
      A(91)=A1
      A(1)=A2
      D(1)=0
      D(91)=0
      H=(A1-A2)/90.
      DO 1000 I=2,90
      D(I)=0
1000  A(I)=A(I-1)+H
      I=2
      K=0
      J1=1
5     DO 2 J=J1,140
      IF(Y(J1).GT.A(I))GOTO3
      IF(Y(J).LT.A(I).AND.Y(J+1).GE.A(I))GOTO4
2     CONTINUE
4      D(I)=THI(J)
       J1=J+1
      GOTO73
3      D(I)=D(I-1)
 73      I=I+1
      IF(I.EQ.92)GOTO77
      GOTO5
77     I2=I-1
 7     DO 70 I=1,91
70    E(I)=0
      WRITE(6,105)(D(I),I=1,91)
105   FORMAT(20F6.3)
      I=I2-1
       E(I2)=THI(J)
       IF(K.EQ.1)J1=J+1
50    DO 20 J=J1,390
      IF(Y(J+1).GT.Y(J))GOTO8
      IF(Y(J+1).LT.A(I).AND.Y(J).GE.A(I))GOTO40
      IF(Y(J).LT.A(I))GOTO41
20    CONTINUE
40     E(I)=THI(J)
      J1=J+1
      GOTO74
41     E(I)=E(I+1)
 74      I=I-1
      IF(I.EQ.0)GOTO8
      GOTO50
  8      E(I)=THI(J)
       IF(I.EQ.0)I=I+1
       I1=I
       DO 9 I=1,91
9     F(I)=0
        WRITE(6,105)(E(I),I=1,91)
       I=I1
       F(I)=THI(J)
       I=I+1
       J1=J+1
15    DO 12 J=J1,399
      IF(Y(J1).GT.A(I))GOTO16
      IF (Y(J).LT.A(I).AND.Y(J+1).GE.A(I))GOTO14
      IF(Y(J+1).LT.Y(J))GOTO17
12    CONTINUE
14      F(I)=THI(J)
      J1=J+1
      IF(J.EQ.399)GOTO17
      GOTO71
16      F(I)=F(I-1)
 71     I=I+1
      IF(I.EQ.92)GOTO17
      GOTO15
17      I2=I
       F(I)=THI(J)
       DO 28 I=I1,91
      IF(K.EQ.1.AND.E(I).EQ.0)E(I)=E(I-1)
      IF(F(I).EQ.0)F(I)=F(I-1)
28     CONTINUE
      WRITE(6,105)(F(I),I=1,91)
      DO 18 I=1,91
      G(I)=F(I)-E(I)
```

```
IV G LEVEL  21                    MAIN                    DATE = 82217          12/02/26

      16    D(I)=D(I)+G(I)
            IF(K.EQ.1)GOTO100
            K=1
            GOTO7
      100    WRITE(6,101)(A(I),D(I),I=1,91)
            DO 102 I=1,91
      102   D(I)=D(I)/6.283
      101      FORMAT(2F12.8)
            WRITE(8,101)(A(I),D(I),I=1,91)
            STOP
            END
```

```
IV G LEVEL  21                    MAX

             SUBROUTINE MAX(X,A,B)
            DIMENSION X(400)
            A=X(1)
            B=A
            DO 1 I=2,400
            IF(A.LT.X(I))A=X(I)
            IF(B.GT.X(I))B=X(I)
      1     CONTINUE
            RETURN
            END
```

```
//HUANG1 JOB (3023,7022,1,1,0),'HUANG',CLASS=A
***
***ROUTE PRINT REMOTE6
// EXEC FORTGCG
XXFORTGCG  PROC DECK=NODECK,LOAD=LOAD,OPTIONS=,COMP=IEYFORTX,
XX              LPARM=MAP,PLOT='DUMMY  ',SUBLIB1='SYS1.FORTLIB',
XX              SUBLIB2='SYS1.FORTLIB',SUBLIB3='SYS1.FORTLIB',
XX              SUBLIB4='SYS1.FORTLIB',SUBLIB5='SYS1.FORTLIB'
XXFORT     EXEC PGM=&COMP,PARM='&DECK,&LOAD,&OPTIONS'
XXSYSPRINT DD   SYSOUT=A
XXSYSPUNCH DD   SYSOUT=B
XXSYSLIN   DD   DSN=&&LIN,UNIT=SYSDA,SPACE=(3100,(152,76),,,ROUND),
XX              DCB=(RECFM=FB,LRECL=80,BLKSIZE=3120),DISP=(,PASS)
//FORT.SYSIN DD *
XXGO       EXEC PGM=LOADER,PARM='&LPARM',COND=(4,LT,FORT)
XXFT05F001 DD   DDNAME=SYSIN
XXFT06F001 DD   SYSOUT=A
XXFT07F001 DD   SYSOUT=B
XXSYSLIB   DD   DDNAME=Z&PLOT
XX         DD   DSN=&SUBLIB1,DISP=SHR
XX         DD   DSN=&SUBLIB2,DISP=SHR
XX         DD   DSN=&SUBLIB3,DISP=SHR
XX         DD   DSN=&SUBLIB4,DISP=SHR
XX         DD   DSN=&SUBLIB5,DISP=SHR
XXSYSLIN   DD   DSN=&&LIN,DISP=(OLD,DELETE)
XX         DD   DDNAME=OBJECT
XXSYSLOUT  DD   SYSOUT=A
XXSYSVECTR DD   &PLOT.DSN=&&VECT,UNIT=SYSDA,DISP=(MOD,PASS),
XX*             SPACE=(TRK,(75,10),RLSE),DCB=BLKSIZE=2400
XXZ        DD   &PLOT.DSN=GRAPHICS.GOULD.LIBRARY,DISP=SHR
XXZDUMMY   DD   DSN=&SUBLIB1,DISP=SHR
//GO.FT02F001 DD UNIT=SYSDA,DSN=UF.B0037000.S28.OB,DISP=OLD
//GO.FT08F001 DD UNIT=SYSDA,DSN=UF.B0037000.S28.HA,DISP=(,CATLG),
//     DCB=(RECFM=FB,LRECL=24,BLKSIZE=2400),SPACE=(2400,(3,1))
//GO.FT03F001 DD UNIT=SYSDA,DSN=UF.B0037000.S28.HB,DISP=(OLD,DELETE)
***EOJ
```